Original Article

Evaluation of microstructural brain changes in post-coronavirus disease 2019 (COVID-19) patients with neurological symptoms: a cross-sectional study

Ibrahim Ibrahim[1]^, Antonín Škoch[1]^, Monika Dezortová[1]^, Theodor Adla[1]^, Vlasta Flusserová[2], Markéta Nagy[1], Irena Douchová[1], Martina Fialová[3]^, Vanda Filová[3]^, Dita Pajuelo[1]^, Markéta Ibrahimová[4]^, Jaroslav Tintěra[1]^

[1]MR Unit, Department of Diagnostic and Interventional Radiology, Institute for Clinical and Experimental Medicine, Prague, Czech Republic; [2]Specialised Outpatient Care Division, Department of Neurology, Institute for Clinical and Experimental Medicine, Prague, Czech Republic; [3]Laboratory Methods Division, Institute for Clinical and Experimental Medicine, Prague, Czech Republic; [4]Laboratory of Immunology, Thomayer University Hospital, Prague, Czech Republic

Contributions: (I) Conception and design: I Ibrahim, J Tintěra; (II) Administrative support: M Nagy, I Douchová, D Pajuelo; (III) Provision of study materials or patients: V Flusserová, M Ibrahimová, M Fialová, V Filová; (IV) Collection and assembly of data: I Ibrahim, M Dezortová; (V) Data analysis and interpretation: I Ibrahim, A Škoch, T Adla; (VI) Manuscript writing: All authors; (VII) Final approval of manuscript: All authors.

Correspondence to: Ibrahim Ibrahim, MSc, PhD. MR Unit, Department of Diagnostic and Interventional Radiology, Institute for Clinical and Experimental Medicine (IKEM), Videnska 1958/9, Prague 14021, Czech Republic. Email: ibrahim.ibrahim@ikem.cz.

Background: Changes in both the vascular system and brain tissues can occur after a prior episode of coronavirus disease 2019 (COVID-19), detectable through modifications in diffusion parameters using magnetic resonance imaging (MRI) techniques. These changes in diffusion parameters may be particularly prominent in highly organized structures such as the corpus callosum (CC), including its major components, which have not been adequately studied following COVID-19 infection. Therefore, the study aimed to evaluate microstructural changes in whole-brain (WB) diffusion, with a specific focus on the CC.

Methods: A total of 101 probands (age range from 18 to 69 years) participated in this retrospective study, consisting of 55 volunteers and 46 post-COVID-19 patients experiencing neurological symptoms. The participants were recruited from April 2022 to September 2023 at the Institute for Clinical and Experimental Medicine in Prague, Czech Republic. All participants underwent MRI examinations on a 3T MR scanner with a diffusion protocol, complemented by additional MRI techniques. Two volunteers and five patients were excluded from the study due to motion artefacts, severe hypoperfusion or the presence of lesions. Participants were selected by a neurologist based on clinical examination and a serological test for COVID-19 antibodies. They were then divided into three groups: a control group of healthy volunteers (n=28), an asymptomatic group (n=25) with a history of infection but no symptoms, and a symptomatic group (n=41) with a history of COVID-19 and neurological symptoms. Symptomatic patients did not exhibit neurological symptoms before contracting COVID-19. Diffusion data underwent eddy current and susceptibility distortion corrections, and fiber tracking was performed using default parameters in DSI studio. Subsequently, various diffusion metrics, were computed within the reconstructed tracts of the WB and CC. To assess the impact of COVID-19 and its associated symptoms on diffusion indices within the white matter of the WB and CC regions, while considering age, we employed a statistical analysis using a

^ ORCID: Ibrahim Ibrahim, 0000-0003-3530-5165; Antonín Škoch, 0000-0002-1739-3256; Monika Dezortová, 0000-0003-0194-1200; Theodor Adla, 0000-0002-0577-1440; Martina Fialová, 0000-0001-5595-3632; Vanda Filová, 0009-0003-5752-4753; Dita Pajuelo, 0000-0001-9046-7736; Markéta Ibrahimová, 0009-0007-5971-4349; Jaroslav Tintěra, 0000-0002-0685-7174.

linear mixed-effects model within the R framework.

Results: Statistical analysis revealed a significant difference in mean diffusivity (MD) between the symptomatic and control groups in the forceps minor (P=0.001) and CC body (P=0.003). In addition to changes in diffusion, alterations in brain perfusion were observed in two post-COVID-19 patients who experienced a severe course. Furthermore, hyperintense lesions were identified in subcortical and deep white matter areas in the vast majority of symptomatic patients.

Conclusions: The main finding of our study was that post-COVID-19 patients exhibit increased MD in the forceps minor and body of the CC. This finding suggests a potential association between microstructural brain changes in post-COVID-19 patients and reported neurological symptoms, with significant implications for research and clinical applications.

Keywords: Post-coronavirus disease 2019 neurological symptoms (post-COVID-19 neurological symptoms); corpus callosum (CC); diffusion magnetic resonance tractography (diffusion MR tractography); microstructural brain changes

Submitted Jan 26, 2024. Accepted for publication Jun 12, 2024. Published online Jul 12, 2024.
doi: 10.21037/qims-24-162
View this article at: https://dx.doi.org/10.21037/qims-24-162

Introduction

Coronavirus disease 2019 (COVID-19) is a highly contagious and severe illness caused by the severe acute respiratory syndrome coronavirus 2 (SARS-CoV-2) virus. It has led to millions of infections and fatalities, precipitating a global pandemic and causing extensive disruptions in the worldwide economy (1,2). While COVID-19 primarily targets the respiratory system (3) it also poses a risk to vital organs such as the brain, heart, kidneys, and others. This can lead to multi-organ dysfunction and persistent medical complications. These complications may persist long after the initial bout of COVID-19, potentially resulting in organ failure or even death. Many individuals who have survived COVID-19 continue to experience a range of neurological and psychological symptoms. These include headaches, fatigue, muscle pain, as well as depression and anxiety, among others (4-7).

Research findings indicate that COVID-19 patients manifest notable alterations in grey matter thickness and contrast in brain tissues. These changes primarily affect the orbitofrontal cortex and parahippocampal gyrus (8), accompanied by hippocampal atrophy and alterations in the corpus callosum (CC) (9). These structural and functional changes are closely linked to cognitive deficits, particularly in attention and memory, as documented in relevant scientific journals (10,11). Additionally, hypoperfusion is predominantly observed in the frontal, parietal, and temporal regions of patients. This observation supports the hypothesis that extensive network dysfunction contributes to cognitive issues following a COVID-19 infection (12).

The most recent research, as summarized in a systematic review, indicates changes in diffusion parameters within white matter (WM) tracts in patients with a history of COVID-19 (13). However, the results from various studies are controversial. Some authors have reported increased mean diffusivity (MD), radial diffusivity (RD), and decreased fractional anisotropy (FA) in WM following COVID-19, as observed in the CC (14,15), while others have reached the opposite conclusion, noting a decrease in MD and axial diffusivity (AD) (16). Furthermore, the relationship between COVID-19 and neurological symptoms remains unclear (17). Changes in diffusion parameters may be particularly notable in well-organized structures such as the CC, including its major components, which have not been thoroughly studied following COVID-19 infection. The CC is one of the largest bundles connecting the two cerebral hemispheres through approximately 200–250 million axonal fibers and play a crucial role in facilitating interhemispheric collaboration (18,19).

The CC typically exhibits high spatial anisotropy under normal conditions, leading to an increased likelihood of detecting more pronounced changes in cases of pathology (20,21). Alterations in both the vascular system and brain tissues (22) can manifest following a prior episode of COVID-19, and they can be identified through modifications in diffusion and perfusion parameters, which can be traced using magnetic resonance imaging (MRI)

techniques during both the acute and chronic phases of the disease (23,24).

Generalized q-sampling imaging (GQI) is a model-free reconstruction technique that provides a quantitative anisotropy (QA) parameter based on the spin distribution function (SDF), defined for each resolved fiber orientation. The GQI algorithm provides both GQI-based metrics such as QA and diffusion tensor imaging (DTI)-based metrics (FA, MD, RD, and AD) (25).

For the aforementioned reasons, our study aims to assess microstructural changes in whole-brain (WB) diffusion, with a specific focus on the CC, utilizing an advanced reconstruction of MR diffusion data and tractography techniques, known as GQI and tractography-based analysis (TBA) (25). We present this article in accordance with the STROBE reporting checklist (available at https://qims.amegroups.com/article/view/10.21037/qims-24-162/rc).

Methods

Study participants

Neurologist-selected patients with history of COVID-19 infection, pre-existing medical conditions, and enduring neurological symptoms, including headaches, fatigue, insomnia, as well as memory and concentration difficulties, underwent a thorough evaluation. This evaluation encompassed clinical examinations, medical histories, and previous assessments for COVID-19 antibody presence, primarily immunoglobulin G (IgG) antibodies in the blood (serology test) to detect evidence of prior infection. The selected patients were adults aged 18–69 years who had experienced persistent neurological symptoms for at least two months following a history of COVID-19 infection. Symptomatic patients did not exhibit neurological symptoms before contracting COVID-19. Subsequently, a control group of volunteers matched in age to the patient group was selected. The participants were recruited from April 2022 to September 2023 at the Institute for Clinical and Experimental Medicine in Prague (IKEM), Czech Republic. The study was conducted in accordance with the Declaration of Helsinki (as revised in 2013) and was approved by the Ethics Committee with multi-center competence of the Institute for Clinical and Experimental Medicine and the Thomayer University Hospital (No. 29451/21; G-21-70). All participants were informed of the purpose of the study and signed a written informed consent form prior to examination.

A total of 101 probands participated in this retrospective study, consisting of 55 volunteers, none exhibited any symptoms or had a significant medical history, and 46 post-COVID patients experiencing neurological symptoms. Subsequently, all participants underwent MRI examinations. Following the recommendation of an experienced radiologist (Dr. Eva Rolencová) with over 30 years of professional experience after visual inspection of the acquired MR data, two volunteers and five patients were excluded from the study due to motion artifacts, severe hypoperfusion or the presence of lesions unrelated to COVID-19 infection. Subsequently, 53 volunteers, who showed no symptoms and had no significant medical history, underwent testing for COVID-19 antibodies.

Detection of antibodies to the nucleocapsid of SARS-CoV-2

All volunteers (n=53) were tested for the specific antibodies to the nucleocapsid of SARS-CoV-2 using the chemiluminescence immunoassay (TestLine Clinical Diagnostics) on the KleeYa analyzer (Stratec). The determination was carried out for antibodies in the immunoglobulin M (IgM) and immunoglobulin A (IgA) classes, indicating the acute phase of infection, and in the IgG class, where the antibodies are anamnestic (26). SARS-CoV-2 infection induces IgG antibodies against the nucleocapsid protein (NP). Healthy volunteers with IgG antibody levels exceeding 22 kU/L (kilounits per liter) were classified as positive, indicating an asymptomatic infection. The results revealed that 25 out of 53 (47.2%) tested positive for antibodies from a previous COVID-19 infection. As a result, the control group essentially consisted of another set of patients who had previously contracted the virus but remained asymptomatic. Based on the results of COVID-19 antibody testing, all participants in this study were categorized into three groups: the control group (c), comprising 28 healthy volunteers without a history of infection; the asymptomatic group (a), consisting of 25 individuals with a history of infection but no symptoms; and the symptomatic group (patients) after COVID-19, with 41 participants who had a history of COVID-19 and neurological symptoms. Detailed information about the proband selection, including the patients' neurological symptoms, is presented in *Figure 1*. The demographic and clinical characteristics of the groups are provided in Table S1 (refer to Appendix 1).

To determine the statistical power, we conducted the following simulation: we generated 1,000 random data

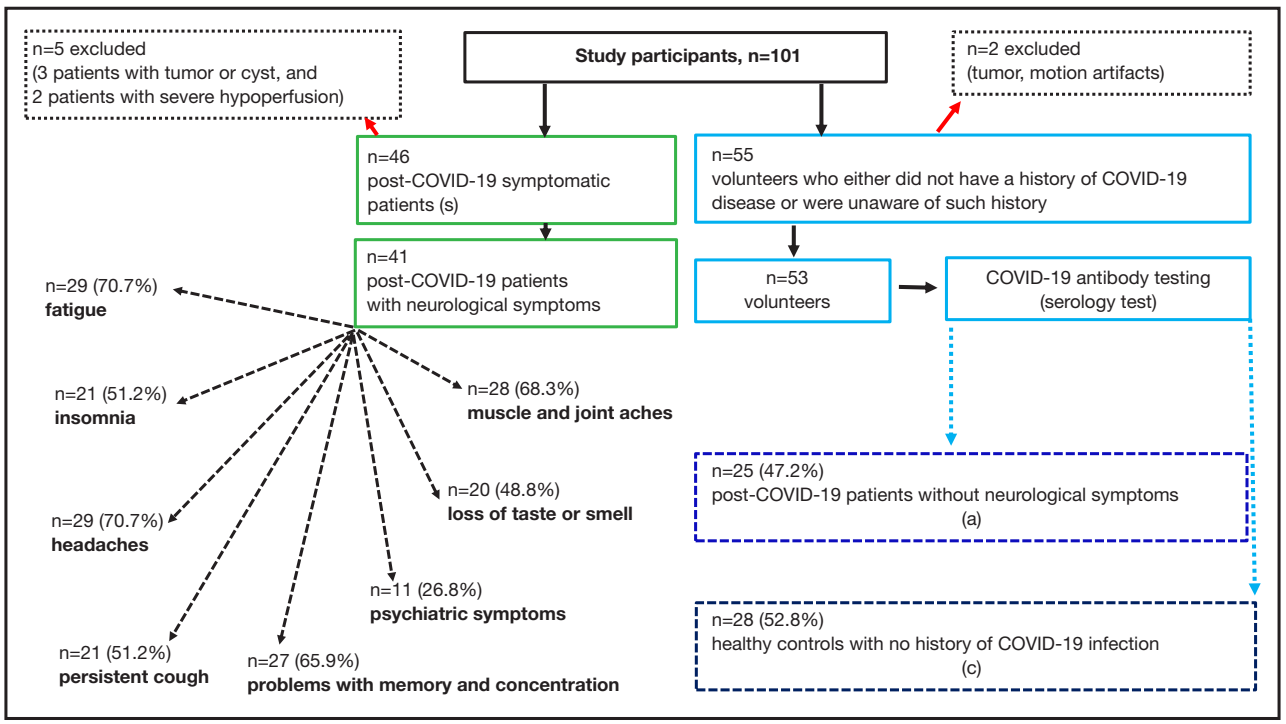

Figure 1 A flowchart illustrating the enrollment of participants, composed of 46 symptomatic post-COVID-19 patients (s) and 55 volunteers with either no history of COVID-19 infection or unawareness of such history. Based on the recommendation of an experienced radiologist after reviewing the MR data, two volunteers and five patients were excluded from the study. Based on COVID-19 antibody testing, volunteers were divided into two groups: asymptomatic patients (a) who had a history of infection without symptoms, and healthy controls (c) with no history of COVID-19 infection. In symptomatic patients, the experienced neurological symptoms are documented. COVID-19, coronavirus disease 2019; MR, magnetic resonance.

realizations for 3 groups with sample sizes of 28, 25, and 41. We used Cohen's d=0.3 to simulate a medium effect size as the difference between groups. Subsequently, we evaluated 1,000 analysis of variance (ANOVA) test P values and calculated the proportion of significant results at P<0.05. The proportion of significant tests, serving as an estimation of power, was found to be 0.578.

MRI acquisition

Participants underwent MRI examinations in the supine position on a 3T MR scanner (Magnetom VIDA 3T, Siemens Healthineers, Germany) equipped with a 64-channel head/neck coil. MR scans were performed according to the optimized measurement protocol for MR diffusion, which is described below:

(I) Diffusion-weighted imaging (DWI) data were obtained using a single-shot echo planar imaging (EPI) sequence, and a q-space diffusion imaging scheme was employed. A total of 122 diffusion samples were obtained with 12 different b-values. The b-values ranged from b=0 to b=4,000 s/mm^2 (b=0, b=450, b=900, b=1,350, b=1,750, b=1,800, b=2,200, b=2,250, b=2,650, b=3,550, b=3,950, and b=4,000). The in-plane resolution and slice thickness were both set at 2 mm.

(II) The diffusion measurement was complemented by additional MRI techniques, including brain perfusion assessment using arterial spin labeling (ASL) technique (27) to detect hypoperfusion, susceptibility-weighted imaging (SWI), used for detecting brain hemorrhages and microbleeds (28), three-dimensional (3D) T2-Fluid Attenuated Inversion Recovery (FLAIR) (29) for detection of abnormalities in the brain, MR angiography (MRA), utilized for visualizing vascular alterations

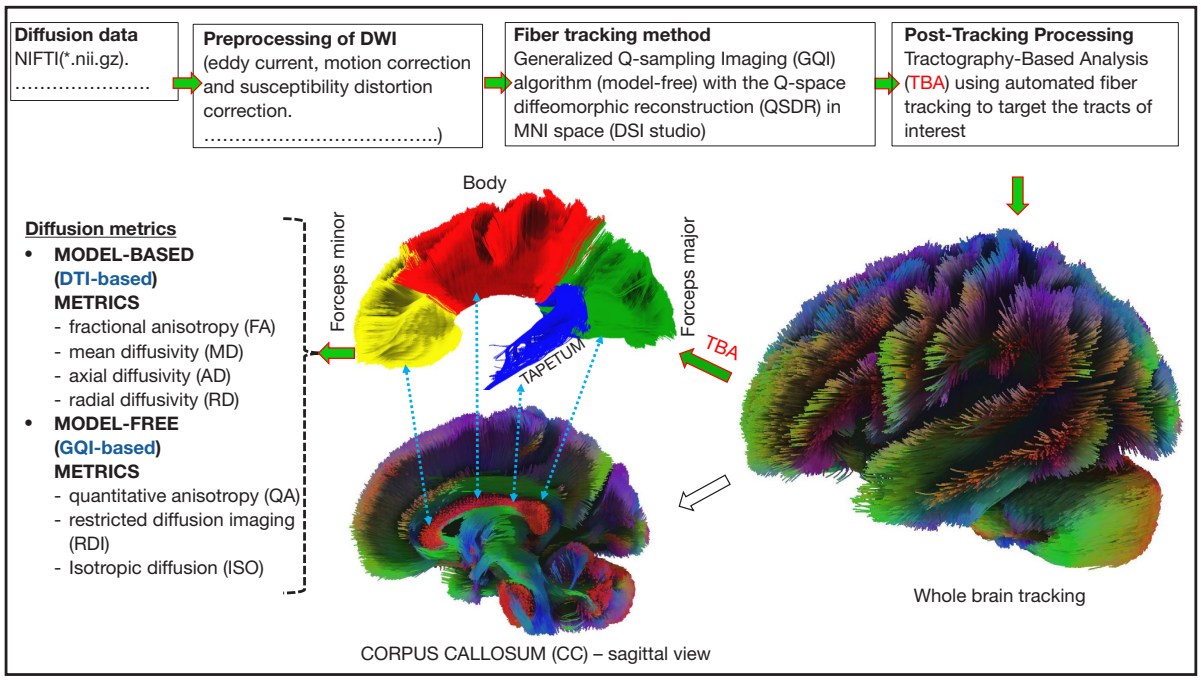

Figure 2 A flowchart describing the preprocessing and post-processing of diffusion data. NIFTI, Neuroimaging Informatics Technology Initiative; DWI, diffusion weighted imaging; MNI, Montreal Neurological Institute; DTI, diffusion tensor imaging.

and malformations (30) and 3D T1 magnetization prepared rapid gradient echo single-shot echo-planar imaging sequence (MPRAGE) for detection structural abnormalities (31). All sequence parameters are summarized in Table S2 (refer to Appendix 1).

Data processing

The susceptibility distortion in diffusion data was corrected using the TOPUP routine, a component of the Tiny FSL package (http://github.com/frankyeh/TinyFSL). This package is a re-compiled version of FSL TOPUP from FMRIB, Oxford, and it has been enhanced with multi-thread support. For this purpose, an additional b=0 image with phase encoding in the reverse direction relative to the main diffusion dataset was acquired (32,33).

For fiber tracking, a deterministic algorithm was employed, complemented by advanced tracking strategies to enhance reproducibility (21). The diffusion data was then reconstructed in the Montreal Neurological Institute (MNI) space using q-space diffeomorphic reconstruction (QSDR) techniques to derive the SDF (25,34). In QSDR, DSI studio (http://dsi-studio.labsolver.org) initially computes the QA mapping in the native space and subsequently standardizes it to the MNI QA map. The diffeomorphic reconstruction's output resolution was 2 mm isotropic, with a diffusion sampling length ratio of 1.25.

Fiber tracking was conducted using the default tracking parameters in the DSI studio.

The anisotropy threshold was chosen randomly. The angular threshold was randomly selected within a range of 15 to 90 degrees. Tracks with lengths less than 20 mm or greater than 200 mm were excluded. The step size was set to match the voxel spacing.

A total of one million seeds were placed. TBA was conducted, using an automated fiber tracking method to reconstruct the entire WM bundles of the brain, with a focus on the CC bundles, including the forceps minor, body, tapetum, and forceps major.

Subsequently, various metrics, such as FA, MD, AD, and RD from DTI, as well as QA, restricted diffusion imaging (RDI), and isotropy (ISO) from GQI, were computed within the reconstructed tracts (*Figure 2*).

The representative multiparametric diffusion maps, encompassing QA, orientation distribution function (ODF), MD, and whole-CC fiber tracking of both a control subject and a post-COVID patient, are presented in *Figure 3*.

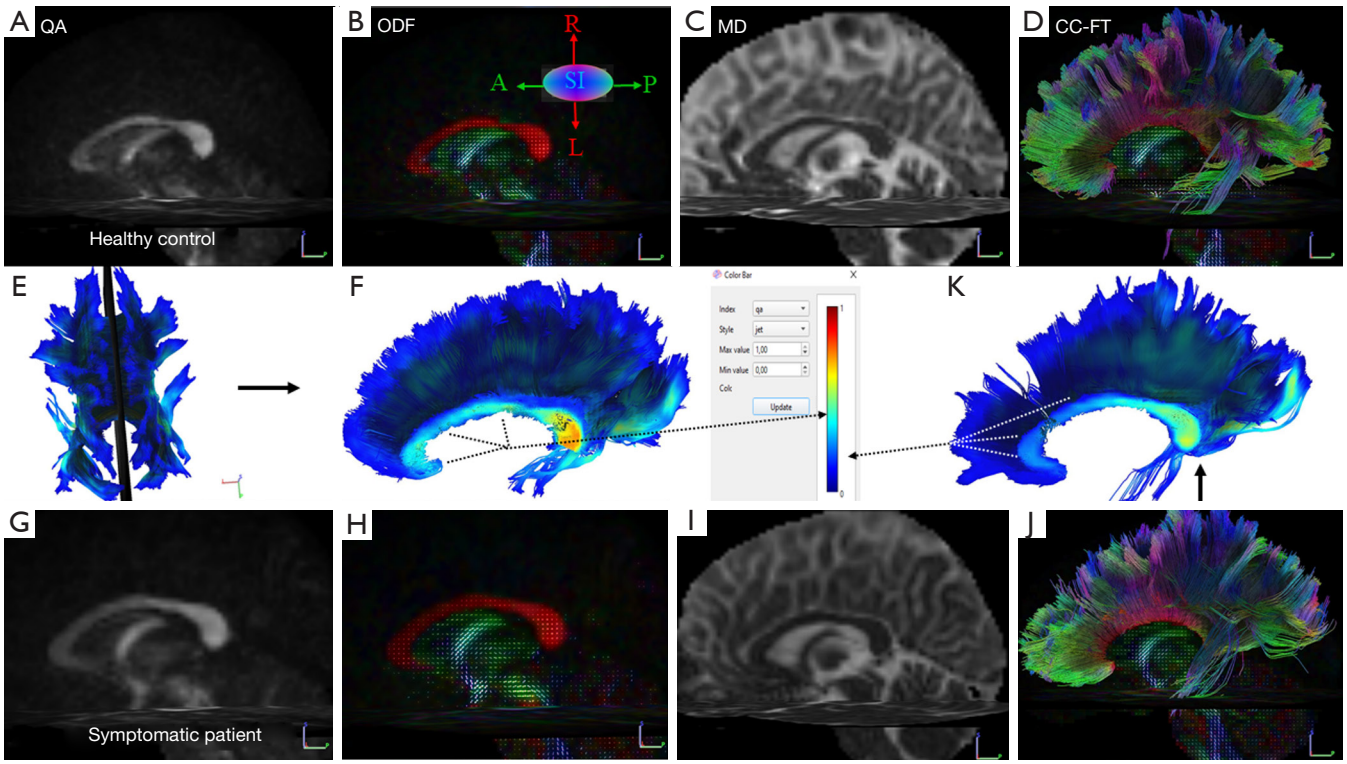

Figure 3 Representative multiparametric diffusion maps in a 45-year-old healthy female control [(A-F) top row] and a 45-year-old symptomatic female patient [(G-K) bottom row]. The color bar (middle row) visually represents the local index of the QA values in the mid-sagittal slice (E) of the corpus callosum fibers, illustrating the differences between the aforementioned control subject (F) and the symptomatic post-COVID-19 patient (K). The directions of the ODF are pseudo-colored: red in the left-right direction (L-R), blue in the superior-inferior direction (S-I), and green in the anterior-posterior (A-P) direction. QA, quantitative anisotropy; ODF, orientation distribution function obtained from q-sampling imaging; MD, mean diffusivity; CC-FT; corpus callosum-fiber tracking; COVID-19, coronavirus disease 2019.

The mean values of DTI-based (FA, MD, AD, and RD) and GQI-based (QA, ISO, and RDI) metrics, along with their corresponding standard deviations, are presented in Tables S3,S4 (refer to Appendix 1). Perfusion map reconstructions, which included relative brain blood flow maps (relCBF), were performed using Siemens' standard software. The assessment of perfusion maps was conducted through a qualitative approach, primarily involving visual inspection by the radiologist (Dr. Eva Rolencová).

Statistical analysis

The initial exploratory data analysis revealed distinct statistical properties in the tapetum, notably a significantly higher variance compared to other structures. This discrepancy could potentially violate the assumption of homoscedasticity in the statistical model. Consequently, it was decided to exclude this structure from further analysis.

To assess the impact of COVID-19 and COVID-related symptoms on diffusion indices in various brain WM regions while accounting for age, we employed a statistical analysis using a linear mixed-effects model within the R framework. The "nlme" package was utilized for this purpose, as documented in the references (35,36). For each dependent variable, such as diffusion indices (FA, MD, AD, RD, QA, RDI, and ISO), a separate model was constructed and assessed.

The explanatory variables in the model included age as a continuous variable (centered around the mean age of the entire group), WM locality (with levels: forceps minor, body of CC, forceps major, and WB), group (with levels: controls, asymptomatic patients, symptomatic patients), and the interaction of structure and group. This interaction term allowed for the individual modeling of dependent

variable values for each structure and group.

Age was treated as a nuisance covariate, and its value was neither evaluated nor used for multiple comparison correction. Furthermore, the study did not explicitly test the effect of WM locality, specifically the differences in diffusion indices between WM regions, as it was not the primary purpose of this research.

The model's results were evaluated by inspecting model residuals, and a Box-Cox transformation was applied to improve the normality of the residuals (37). The optimal lambda for the Box-Cox transformation was determined by assessing P values derived from the Shapiro-Wilk test applied to the model residuals, and the lambda corresponding to the maximal P value of the test was selected and used.

Non-significant terms were removed from the models using the Akaike information criterion. The exclusion of specific terms owing to their lack of statistical significance is a standard approach for simplifying models in statistical analysis, aiding in refining the interpretation of the results.

For the remaining terms involving group and group: locality interaction after model simplification, ANOVA-like P values of likelihood ratio tests were computed to determine the overall significance of these terms in the model. These P values were subjected to multiple comparison correction using the Holm method (38). Given the significance of the interaction term in the likelihood ratio test for MD, a post-hoc analysis was performed on this model to elucidate the specific behavior of the terms that correspond to the relationship between MD and group within particular brain regions. A P value <0.05 with two-sided test was considered statistically significant.

Results

The boxplots in *Figure 4* depict diffusion indices across different subject groups and WM locations. These plots illustrate a trend of increasing values in MD, RD, and AD, along with a decrease in FA, when comparing controls, asymptomatic, and symptomatic patients. However, it's important to note that this trend is not consistently observed across all regions. Boxplots describing the remaining diffusion indices for the GQI-based metrics (QA, RDI and ISO) are shown in *Figure 5*.

In the linear mixed-effects model analysis, the process of model simplification by removing of non-significant terms resulted in the exclusion of group and interaction terms in RDI and ISO, along with the interaction term in QA. The ANOVA-like P values for the remaining terms (MD, AD, RD, and QA) are detailed in *Table 1* both before and after correction for multiple comparisons. Post-correction, only the structure: group-interaction term of MD remains statistically significant, indicating a noteworthy difference in MD concerning the group dependency across WM localities.

A post-hoc analysis of MD using general hypothesis test (implemented in R package multcomp) showed significant difference between control and symptomatic patients in the forceps minor (P=0.001), body of the CC (P=0.003), whereas such a difference is not observed in the Forceps major (P=0.7) and WB (P=0.46) (see the corresponding boxplot in *Figure 4*).

For other diffusion indices (FA, AD, RD, QA, RDI, and ISO), the ANOVA-like P values for terms after correction are not significant or were removed during the simplification step, indicating that the results in the graphs should be interpreted as non-significant trends.

In terms of brain perfusion, only two out of the six patients who experienced a severe course requiring hospitalization and treatment with oxygen therapy exhibited hypoperfusion in the right hemisphere, particularly in the temporal and frontal regions. They were subsequently excluded from the study to eliminate potential effects on the outcome of the diffusion data analysis. The remaining four hospitalized patients had similar diffusion and perfusion results to the other patients; therefore, they were included in the study. A representative regional cerebral blood flow (rCBF) map illustrating perfusion, along with corresponding results from complementary MR images, is shown in *Figure 6*. The remaining patients, excluding the two previously referenced, showed no signs of hypoperfusion, microbleeding, or vascular abnormalities.

In contrast to perfusion, hyperintense lesions in the subcortical and deep WM were observed in the majority (70.7%) of symptomatic post-COVID-19 patients, as seen in FLAIR images with corresponding findings on MPRAGE images (*Figure 7*).

Discussion

Understanding microstructural changes in the brain, notably within areas such as the CC, which is an emerging area of research, could provide insights into the neurological impacts of COVID-19. The observed trend of higher MD values in symptomatic subjects compared to controls in our study suggests changes in WM microstructure that may be

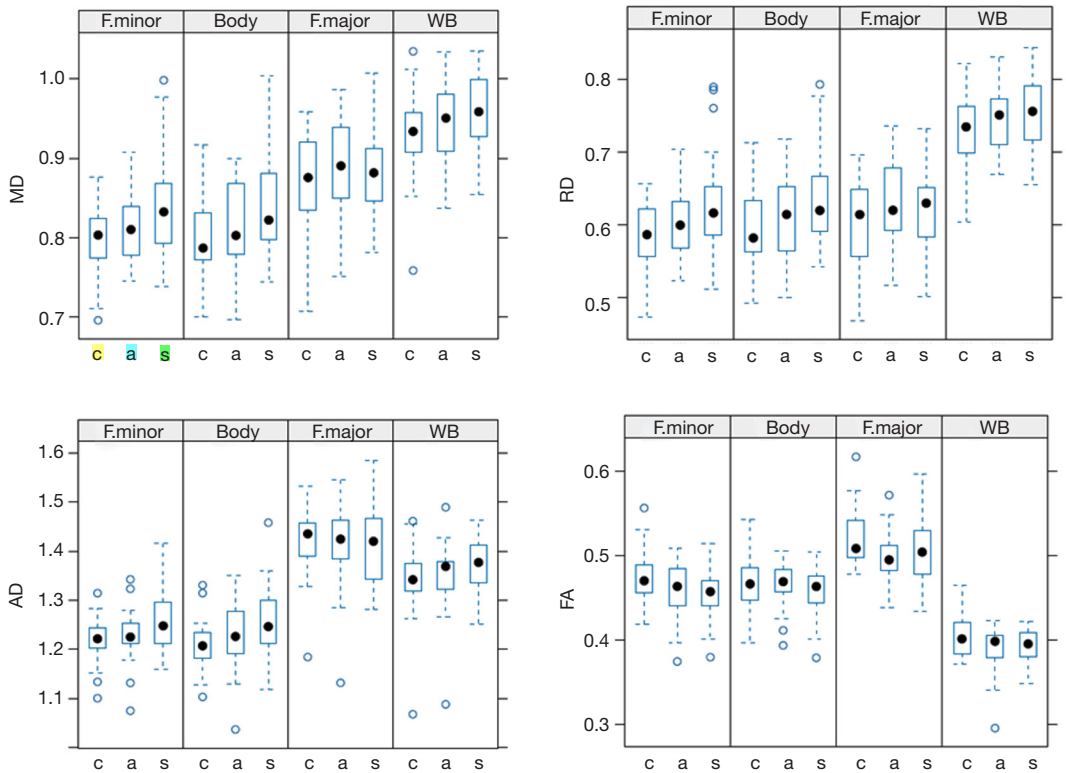

Figure 4 The trend of increasing MD values when comparing controls, asymptomatic, and symptomatic patients. A post-hoc analysis showed significant differences between control and symptomatic patients in the forceps minor (P=0.001) and body of the CC (P=0.003), but not in the Forceps major (P=0.7) or WB (P=0.46). Similar trends were observed in other DTI-based metrics: RD and AD values increased, while FA values decreased, although these changes were not statistically significant. • full circles represent median values; while open circles ° denote outlier values. The MD, RD, and AD are expressed in units of $mm^2/s \times 10^{-3}$. MD, mean diffusivity; F. minor, forceps minor; F. major, forceps major of the CC; WB, whole-brain; c, controls; a, asymptomatic patients; s, symptomatic patients; RD, radial diffusivity; AD, axial diffusivity; FA, fractional anisotropy; CC, corpus callosum; DTI, diffusion tensor imaging.

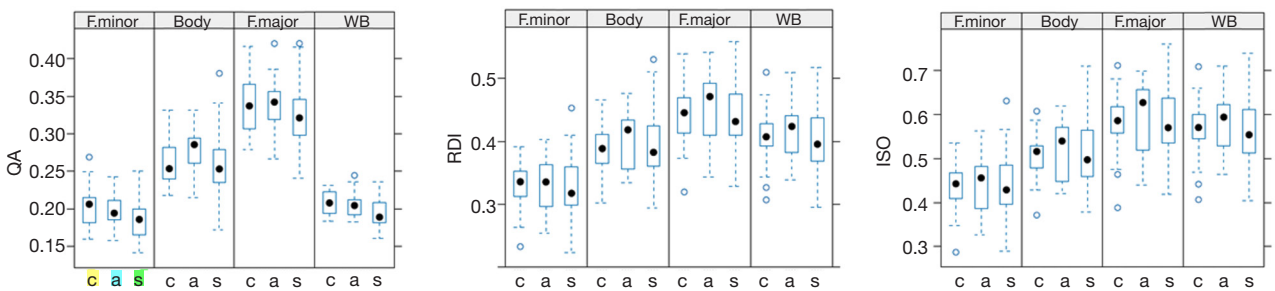

Figure 5 The trend of decreasing mean QA, RDI, and ISO imaging values when comparing controls, asymptomatic, and symptomatic patients. Nevertheless, these changes between control and symptomatic patients were not statistically significant (P>0.05). • full circles represent median values; while open circles ° denote outlier values. QA, quantitative anisotropy; F. minor, forceps minor; F. major, forceps major of the corpus callosum; WB, whole brain; c, controls; a, asymptomatic patients; s, symptomatic patients; RDI, restricted diffusion imaging; ISO, isotropy.

Table 1 The ANOVA-like P values for the terms (MD, AD, RD, and QA) both before and after correction for multiple comparisons

Terms (diffusion metrics)	Uncorrected P	Corrected P
MD group	0.0387	0.1548
MD interaction	0.0032	0.0224
AD group	0.0967	0.1548
AD interaction	0.0135	0.0810
RD group	0.0401	0.1548
RD interaction	0.0204	0.1020
QA group	0.0494	0.1548

The group-interaction term of MD is statistically significant (P=0.0224), suggesting a noteworthy difference in MD concerning the group dependency across white matter localities. ANOVA, analysis of variance; MD, mean diffusivity; AD, axial diffusivity; RD, radial diffusivity; QA, quantitative anisotropy.

associated with neurological conditions. MD is recognized as a sensitive indicator of microstructural changes in the brain and can reflect variations within both the intra- and extracellular space (39,40). Consequently, MD values may be influenced by disease-related pathophysiological processes that affect the barriers restricting diffusion, leading to changes in the cellular microenvironment. Additionally, recent research has reported evident disruption of the blood-brain barrier (BBB) during acute infection and in patients experiencing long-term cognitive impairment due to COVID-19 (41).

Our results are consistent with the literature suggesting increased MD, RD, and AD, along with a decrease in FA in the WM tract within the CC among patients with a history of COVID-19 (13). In contrast to several published case reports that have shown cytotoxic lesions or encephalitis

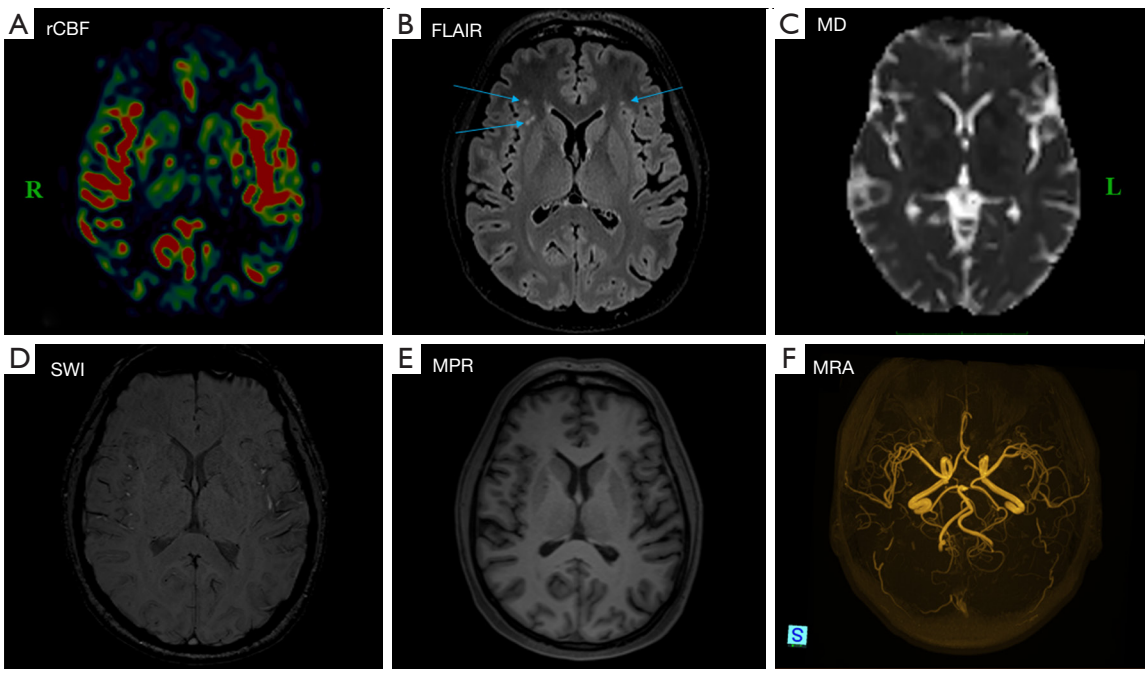

Figure 6 A representative map (A) of normal rCBF in a 47-year-old symptomatic female patient is provided, along with the corresponding results from complementary MR images (B-F). The arrows indicate hyperintense lesions observed following a history of COVID-19 infection. Apart from the lesions identified on 3D T2-FLAIR images (B), there are no abnormal findings noted on MD, SWI, MPR gradient echo single-shot echo-planar imaging sequence, or MRA images (C-F). L indicates left, and R indicates right. rCBF, regional cerebral blood flow; FLAIR, fluid attenuated inversion recovery; MD, mean diffusivity; SWI, susceptibility-weighted imaging; MPR, magnetization prepared rapid; MRA, MR angiography; MR, magnetic resonance; COVID-19, coronavirus disease 2019; 3D, three-dimensional.

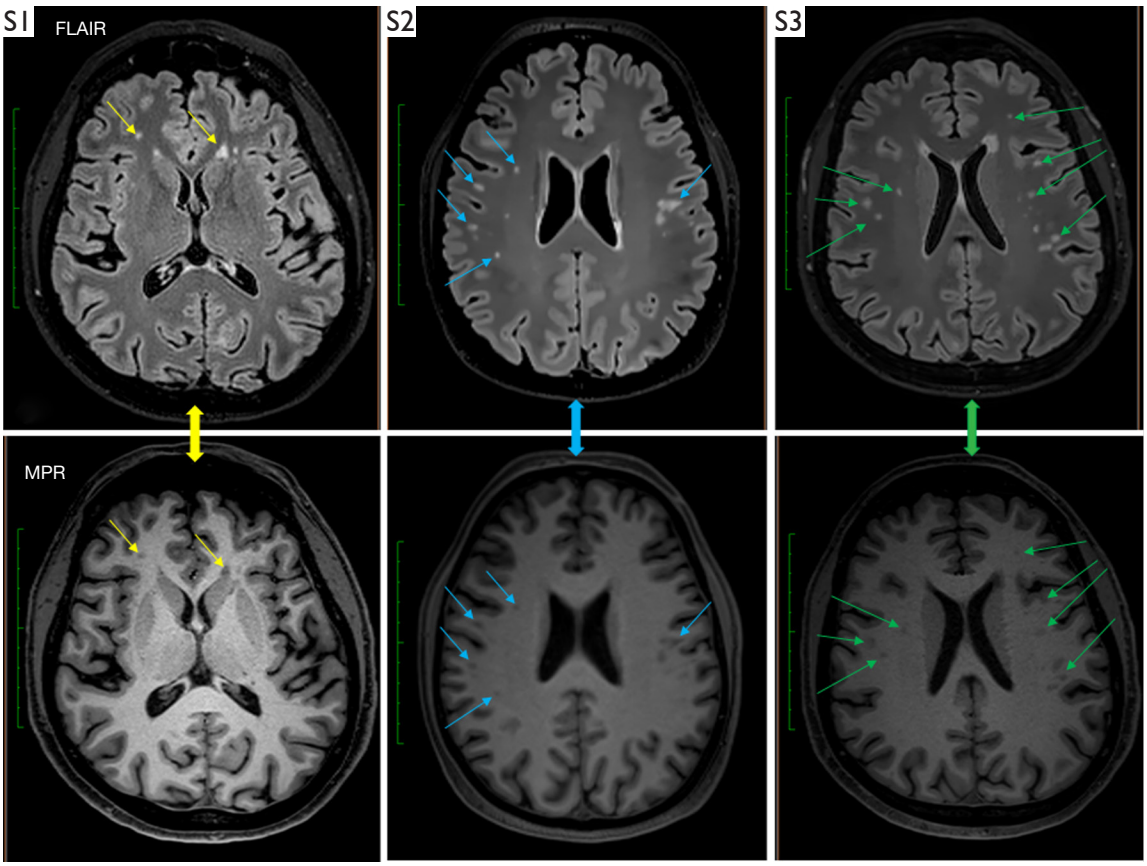

Figure 7 Examples of hyperintense lesions on FLAIR images in three symptomatic patients: a 48-year-old man (S1), a 45-year-old woman (S2), and a 49-year-old woman (S3), along with corresponding findings on MPR images. The arrows indicate hyperintense lesions observed following a history of COVID-19 infection. FLAIR, fluid attenuated inversion recovery; MPR, magnetization prepared rapid; COVID-19, coronavirus disease 2019.

in the splenium of the CC (42-44), we did not observe any lesions in the CC in our patients. These lesions are not specific to COVID-19 disease and are linked to various categories of diseases, including toxic or drug-related causes, metabolic disorders, vascular issues, infections, traumatic events, and neoplastic conditions (45).

The observation of a significant changes in both the forceps minor and body of the CC, is supported by studies recognizing these areas as key regions where MD differences manifest, underscoring their relevance in disease characterization and prognosis (20,46,47). This phenomenon often signifies alterations in WM microstructure associated with neurological conditions (48-50), consistently reinforces the importance of MD as a reliable marker for differentiating between groups. However, it should be noted that the observed significant differences in MD are limited to specific WM regions, such as forceps minor and body of the CC. This suggests that the neurological impact of COVID-19 may not be uniform across the entire brain. The results of our study also indicate that in cases of severe disease, brain hypoperfusion may occur. This was observed in the temporal and frontal regions of the right hemisphere in two out of the six hospitalized post-COVID-19 patients we examined. While it is widely accepted that frontal regions, particularly the prefrontal cortex, play a pivotal role in cognitive functions such as decision-making, problem-solving, emotional regulation, working memory, and various others (51), the direct link between COVID-19 related neurological symptoms and diffusion changes in the WM of these regions is still a topic of ongoing research and debate. This connection is not fully understood. Neurological symptoms

in COVID-19 patients can manifest due to a variety of reasons, including direct viral effects, viral dose, vascular issues, inflammation, and the unique immune response of each individual (52,53).

Another noteworthy finding in our study is that 47.2% of individuals among the volunteers, identified as asymptomatic through antibody testing, leads to a significant conclusion. This suggests that a substantial portion of the population had encountered the virus and developed an immunological response. Additionally, a significant observation among post-COVID-19 patients is the outcome of proton MR spectroscopy, indicating a noticeable difference in choline concentration within the CC when compared to control groups (54). Choline is known as a key factor in cell membrane formation and is essential for normal nervous system function. It serves as a precursor to the neurotransmitter acetylcholine, playing a crucial role in signal transmission between neurons and contributing to processes associated with cognitive function (55).

It is important to note that, although our study lacks a longitudinal design (patients were not scanned before contracting COVID-19), patients did not exhibit these specific neurological symptoms before their COVID-19 infection. The observed changes in diffusion parameters and brain perfusion in some patients following severe COVID-19, along with the identification of hyperintense lesions in subcortical and deep WM areas in 70.7% of our patients following COVID-19 (as shown in *Figures 6*,*7*), may indicate microstructural brain changes. These abnormalities could potentially be linked to the neurological symptoms reported by these patients.

Our study has limitations, such as variability in patients' symptoms and severities, as well as the exclusive use of qualitative evaluation for assessing perfusion maps.

Nevertheless, our findings offer important insights into the variations in WM microstructure among different subject groups, namely control, asymptomatic, and symptomatic individuals. These findings provide a foundation for understanding how brain WM microstructure differs across these groups, which can have significant implications for both research and clinical applications. Evaluation and understanding microstructural brain changes, particularly in the CC, using multiparametric MR methods in post-COVID patients, is a crucial avenue of research with potential implications for patient care, public health, and our comprehension of the neurological effects of the virus.

Conclusions

Individuals recovering from COVID-19 exhibit noticeable modifications in the WM of the brain, particularly affecting the forceps minor and the body of the CC. Observed changes in WM, along with the presence of numerous hyperintense lesions and alterations in brain perfusion in some patients, suggest a possible correlation with the neurological symptoms reported by these individuals.

Acknowledgments

We would like to thank Dr. Milan Hájek, Dr. Eva Rolencová, and Dr. Jan Kovář for all their help in solving the grant project.

Funding: The study was supported by Ministry of Health of the Czech Republic (No. AZV NU22-A-124) and MH CZ - Conceptual Developmental Organization (Institute for Clinical and Experimental Medicine - IKEM) (IN 00023001).

Footnote

Reporting Checklist: The authors have completed the STROBE reporting checklist. Available at https://qims.amegroups.com/article/view/10.21037/qims-24-162/rc

Conflicts of Interest: All authors have completed the ICMJE uniform disclosure form (available at https://qims.amegroups.com/article/view/10.21037/qims-24-162/coif). The authors have no conflicts of interest to declare.

Ethical Statement: The authors are accountable for all aspects of the work in ensuring that questions related to the accuracy or integrity of any part of the work are appropriately investigated and resolved. The study was conducted in accordance with the Declaration of Helsinki (as revised in 2013) and was approved by the Ethics Committee with multi-center competence of the Institute for Clinical and Experimental Medicine and the Thomayer University Hospital (No. 29451/21; G-21-70). All participants were informed of the purpose of the study and signed a written informed consent form prior to examination.

References

1. Mallah SI, Ghorab OK, Al-Salmi S, Abdellatif OS, Tharmaratnam T, Iskandar MA, Sefen JAN, Sidhu P, Atallah B, El-Lababidi R, Al-Qahtani M. COVID-19: breaking down a global health crisis. Ann Clin Microbiol Antimicrob 2021;20:35.
2. Shang Y, Li H, Zhang R. Effects of Pandemic Outbreak on Economies: Evidence From Business History Context. Front Public Health 2021;9:632043.
3. Greffier J, Hoballah A, Sadate A, de Oliveira F, Claret PG, de Forges H, Loubet P, Mauboussin JM, Hamard A, Beregi JP, Frandon J. Ultra-low-dose chest CT performance for the detection of viral pneumonia patterns during the COVID-19 outbreak period: a monocentric experience. Quant Imaging Med Surg 2021;11:3190-9.
4. Sher L. Post-COVID syndrome and suicide risk. QJM 2021;114:95-8.
5. Liu JWTW, de Luca RD, Mello Neto HO, Barcellos I. Post-COVID-19 Syndrome? New daily persistent headache in the aftermath of COVID-19. Arq Neuropsiquiatr 2020;78:753-4.
6. Revzin MV, Raza S, Warshawsky R, D'Agostino C, Srivastava NC, Bader AS, Malhotra A, Patel RD, Chen K, Kyriakakos C, Pellerito JS. Multisystem Imaging Manifestations of COVID-19, Part 1: Viral Pathogenesis and Pulmonary and Vascular System Complications. Radiographics 2020;40:1574-99.
7. Revzin MV, Raza S, Srivastava NC, Warshawsky R, D'Agostino C, Malhotra A, Bader AS, Patel RD, Chen K, Kyriakakos C, Pellerito JS. Multisystem Imaging Manifestations of COVID-19, Part 2: From Cardiac Complications to Pediatric Manifestations. Radiographics 2020;40:1866-92.
8. Douaud G, Lee S, Alfaro-Almagro F, Arthofer C, Wang C, McCarthy P, Lange F, Andersson JLR, Griffanti L, Duff E, Jbabdi S, Taschler B, Keating P, Winkler AM, Collins R, Matthews PM, Allen N, Miller KL, Nichols TE, Smith SM. SARS-CoV-2 is associated with changes in brain structure in UK Biobank. Nature 2022;604:697-707.
9. Huang S, Zhou Z, Yang D, Zhao W, Zeng M, Xie X, Du Y, Jiang Y, Zhou X, Yang W, Guo H, Sun H, Liu P, Liu J, Luo H, Liu J. Persistent white matter changes in recovered COVID-19 patients at the 1-year follow-up. Brain 2022;145:1830-8.
10. Klironomos S, Tzortzakakis A, Kits A, Öhberg C, Kollia E, Ahoromazdae A, Almqvist H, Aspelin Å, Martin H, Ouellette R, Al-Saadi J, Hasselberg M, Haghgou M, Pedersen M, Petersson S, Finnsson J, Lundberg J, Falk Delgado A, Granberg T. Nervous System Involvement in Coronavirus Disease 2019: Results from a Retrospective Consecutive Neuroimaging Cohort. Radiology 2020;297:E324-34.
11. Díez-Cirarda M, Yus-Fuertes M, Sanchez-Sanchez R, Gonzalez-Rosa JJ, Gonzalez-Escamilla G, Gil-Martínez L, et al. Hippocampal subfield abnormalities and biomarkers of pathologic brain changes: from SARS-CoV-2 acute infection to post-COVID syndrome. EBioMedicine 2023;94:104711.
12. Ajčević M, Iscra K, Furlanis G, Michelutti M, Miladinović A, Buoite Stella A, Ukmar M, Cova MA, Accardo A, Manganotti P. Cerebral hypoperfusion in post-COVID-19 cognitively impaired subjects revealed by arterial spin labeling MRI. Sci Rep 2023;13:5808.
13. Mohammadi S, Ghaderi S. Post-COVID-19 conditions: a systematic review on advanced magnetic resonance neuroimaging findings. Neurol Sci 2024;45:1815-33.
14. Paolini M, Palladini M, Mazza MG, Colombo F, Vai B, Rovere-Querini P, Falini A, Poletti S, Benedetti F. Brain correlates of subjective cognitive complaints in COVID-19 survivors: A multimodal magnetic resonance imaging study. Eur Neuropsychopharmacol 2023;68:1-10.
15. Clouston S, Huang C, Ying J, Sekendiz Z, Kritikos M, Fontana A, Bangiyev L, Luft B. Neuroinflammatory imaging markers in white matter: insights into the cerebral consequences of post-acute sequelae of COVID-19 (PASC). Res Sq [Preprint] 2024;rs.3.rs-3760289.
16. Díez-Cirarda M, Yus M, Gómez-Ruiz N, Polidura C, Gil-Martínez L, Delgado-Alonso C, Jorquera M, Gómez-Pinedo U, Matias-Guiu J, Arrazola J, Matias-Guiu JA. Multimodal neuroimaging in post-COVID syndrome and correlation with cognition. Brain 2023;146:2142-52.
17. Molaverdi G, Kamal Z, Safavi M, Shafiee A, Mozhgani SH, Ghobadi MZ, Goudarzvand M. Neurological complications after COVID-19: A narrative review. eNeurologicalSci 2023;33:100485.
18. Fitsiori A, Nguyen D, Karentzos A, Delavelle J, Vargas MI. The corpus callosum: white matter or terra incognita. Br J Radiol 2011;84:5-18.
19. Filippi CG, Cauley KA. Lesions of the corpus callosum

and other commissural fibers: diffusion tensor studies. Semin Ultrasound CT MR 2014;35:445-58.
20. Planchuelo-Gómez Á, García-Azorín D, Guerrero ÁL, Rodríguez M, Aja-Fernández S, de Luis-García R. Structural brain changes in patients with persistent headache after COVID-19 resolution. J Neurol 2023;270:13-31.
21. Yeh FC, Verstynen TD, Wang Y, Fernández-Miranda JC, Tseng WY. Deterministic diffusion fiber tracking improved by quantitative anisotropy. PLoS One 2013;8:e80713.
22. Ardellier FD, Baloglu S, Sokolska M, Noblet V, Lersy F, Collange O, et al. Cerebral perfusion using ASL in patients with COVID-19 and neurological manifestations: A retrospective multicenter observational study. J Neuroradiol 2023;50:470-81.
23. Sun C, Liu X, Bao C, Wei F, Gong Y, Li Y, Liu J. Advanced non-invasive MRI of neuroplasticity in ischemic stroke: Techniques and applications. Life Sci 2020;261:118365.
24. Martinez-Heras E, Grussu F, Prados F, Solana E, Llufriu S. Diffusion-Weighted Imaging: Recent Advances and Applications. Semin Ultrasound CT MR 2021;42:490-506.
25. Yeh FC, Wedeen VJ, Tseng WY. Generalized q-sampling imaging. IEEE Trans Med Imaging 2010;29:1626-35.
26. Fu Y, Pan Y, Li Z, Li Y. The Utility of Specific Antibodies Against SARS-CoV-2 in Laboratory Diagnosis. Front Microbiol 2020;11:603058.
27. Jaganmohan D, Pan S, Kesavadas C, Thomas B. A pictorial review of brain arterial spin labelling artefacts and their potential remedies in clinical studies. Neuroradiol J 2021;34:154-68.
28. Haller S, Haacke EM, Thurnher MM, Barkhof F. Susceptibility-weighted Imaging: Technical Essentials and Clinical Neurologic Applications. Radiology 2021;299:3-26.
29. Gwo CY, Zhu DC, Zhang R. Brain white matter hyperintensity lesion characterization in 3D T(2) fluid-attenuated inversion recovery magnetic resonance images: Shape, texture, and their correlations with potential growth. Front Neurosci 2022;16:1028929.
30. Guest W, Krings T. Brain Arteriovenous Malformations: The Role of Imaging in Treatment Planning and Monitoring Response. Neuroimaging Clin N Am 2021;31:205-22.
31. Mugler JP 3rd, Brookeman JR. Three-dimensional magnetization-prepared rapid gradient-echo imaging (3D MP RAGE). Magn Reson Med 1990;15:152-7.
32. Andersson JL, Skare S, Ashburner J. How to correct susceptibility distortions in spin-echo echo-planar images: application to diffusion tensor imaging. Neuroimage 2003;20:870-88.
33. Smith SM, Jenkinson M, Woolrich MW, Beckmann CF, Behrens TE, Johansen-Berg H, Bannister PR, De Luca M, Drobnjak I, Flitney DE, Niazy RK, Saunders J, Vickers J, Zhang Y, De Stefano N, Brady JM, Matthews PM. Advances in functional and structural MR image analysis and implementation as FSL. Neuroimage 2004;23 Suppl 1:S208-19.
34. Yeh FC, Tseng WY. NTU-90: a high angular resolution brain atlas constructed by q-space diffeomorphic reconstruction. Neuroimage 2011;58:91-9.
35. Pinheiro J, Bates D, R Core Team. nlme: Linear and Nonlinear Mixed Effects Models 2023 R package version 3.1-163. Available online: https://cran.r-project.org/web/packages/nlme/nlme.pdf
36. Pinheiro JC, Bates DM. Mixed-Effects Models in S and S-PLUS. Springer, New York, 2000.
37. Box GEP, Cox DR. An Analysis of Transformations. Journal of the Royal Statistical Society 1964;26:211-52.
38. Holm, S. A simple sequentially rejective multiple test procedure. Scandinavian Journal of Statistics 1979;6:5-70.
39. Alexander AL, Lee JE, Lazar M, Field AS. Diffusion tensor imaging of the brain. Neurotherapeutics 2007;4:316-29.
40. Liang H, Ernst T, Oishi K, Ryan MC, Herskovits E, Cunningham E, Wilson E, Kottilil S, Chang L. Abnormal brain diffusivity in participants with persistent neuropsychiatric symptoms after COVID-19. NeuroImmune Pharm Ther 2023;2:37-48.
41. Greene C, Connolly R, Brennan D, Laffan A, O'Keeffe E, Zaporojan L, O'Callaghan J, Thomson B, Connolly E, Argue R, Meaney JFM, Martin-Loeches I, Long A, Cheallaigh CN, Conlon N, Doherty CP, Campbell M. Blood-brain barrier disruption and sustained systemic inflammation in individuals with long COVID-associated cognitive impairment. Nat Neurosci 2024;27:421-32.
42. Tanwar M, Singhal A, Alizadeh M, Sotoudeh H. Magnetic Resonance Imaging (MRI) Findings in COVID-19 Associated Encephalitis. Neurol Int 2023;15:55-68.
43. Kubo M, Kubo K, Kobayashi KI, Komiya N. Non-severe COVID-19 complicated by cytotoxic lesions of the corpus callosum (mild encephalitis/encephalopathy with a reversible splenial lesion): a case report and literature review. Int J Infect Dis 2022;125:1-9.
44. Ohara H, Shimizu H, Kasamatsu T, Kajita A, Uno K, Lai KW, Vellingiri B, Sugie K, Kinoshita M. Cytotoxic lesions of the corpus callosum after COVID-19 vaccination.

Neuroradiology 2022;64:2085-9.
45. Moors S, Nakhostin D, Ilchenko D, Kulcsar Z, Starkey J, Winklhofer S, Ineichen BV. Cytotoxic lesions of the corpus callosum: a systematic review. Eur Radiol 2023. [Epub ahead of print]. doi: 10.1007/s00330-023-10524-3.
46. Campabadal A, Oltra J, Junqué C, Guillen N, Botí MÁ, Sala-Llonch R, Monté-Rubio GC, Lledó G, Bargalló N, Rami L, Sánchez-Valle R, Segura B. Structural brain changes in post-acute COVID-19 patients with persistent olfactory dysfunction. Ann Clin Transl Neurol 2023;10:195-203.
47. Teller N, Chad JA, Wong A, Gunraj H, Ji X, Goubran M, et al. Feasibility of diffusion-tensor and correlated diffusion imaging for studying white-matter microstructural abnormalities: Application in COVID-19. Hum Brain Mapp 2023;44:3998-4010.
48. Shan D, Li S, Xu R, Nie G, Xie Y, Han J, Gao X, Zheng Y, Xu Z, Dai Z. Post-COVID-19 human memory impairment: A PRISMA-based systematic review of evidence from brain imaging studies. Front Aging Neurosci 2022;14:1077384.
49. Afsahi AM, Norbash AM, Syed SF, Sedaghat M, Afsahi G, Shahidi R, Tajabadi Z, Bagherzadeh-Fard M, Karami S, Yarahmadi P, Shirdel S, Asgarzadeh A, Baradaran M, Khalaj F, Sadeghsalehi H, Fotouhi M, Habibi MA, Jang H, Alavi A, Sedaghat S. Brain MRI findings in neurologically symptomatic COVID-19 patients: a systematic review and meta-analysis. J Neurol 2023;270:5131-54.
50. Bispo DDC, Brandão PRP, Pereira DA, Maluf FB, Dias BA, Paranhos HR, von Glehn F, de Oliveira ACP, Regattieri NAT, Silva LS, Yasuda CL, Soares AASM, Descoteaux M. Brain microstructural changes and fatigue after COVID-19. Front Neurol 2022;13:1029302.
51. Jones DT, Graff-Radford J. Executive Dysfunction and the Prefrontal Cortex. Continuum (Minneap Minn) 2021;27:1586-601.
52. García LF. Immune Response, Inflammation, and the Clinical Spectrum of COVID-19. Front Immunol 2020;11:1441.
53. Shi Y, Wang Y, Shao C, Huang J, Gan J, Huang X, Bucci E, Piacentini M, Ippolito G, Melino G. COVID-19 infection: the perspectives on immune responses. Cell Death Differ 2020;27:1451-4.
54. Pajuelo D, Dezortova M, Hajek M, Ibrahimova M, Ibrahim I. Metabolic changes assessed by 1H MR spectroscopy in the corpus callosum of post-COVID patients. MAGMA 2024. [Epub ahead of print]. doi: 10.1007/s10334-024-01171-w.
55. Kansakar U, Trimarco V, Mone P, Varzideh F, Lombardi A, Santulli G. Choline supplements: An update. Front Endocrinol (Lausanne) 2023;14:1148166.

Cite this article as: Ibrahim I, Škoch A, Dezortová M, Adla T, Flusserová V, Nagy M, Douchová I, Fialová M, Filová V, Pajuelo D, Ibrahimová M, Tintěra J. Evaluation of microstructural brain changes in post-coronavirus disease 2019 (COVID-19) patients with neurological symptoms: a cross-sectional study. Quant Imaging Med Surg 2024;14(8):5499-5512. doi: 10.21037/qims-24-162

